

## Resonant x-ray scattering in $\text{La}_{1-x}\text{Sr}_{1+x}\text{MnO}_4$ ( $x \geq 0.5$ ): Incommensurate-lattice modulation vs. Charge-stripe models

G Subías<sup>1</sup>, J García<sup>1</sup>, J Herrero-Martín<sup>2</sup>, J Blasco<sup>1</sup> and M C Sánchez<sup>1</sup>

<sup>1</sup> Instituto de Ciencia de Materiales de Aragón, Departamento de Física de la Materia Condensada, CSIC-Universidad de Zaragoza, Pedro Cerbuna 12, 50009-Zaragoza, Spain

<sup>2</sup> ALBA Synchrotron Radiation Facility, Crta. BP 1413 Km 3.3, 08290, Cerdanyola del Vallès, Barcelona, Spain

E-mail: gloria@unizar.es

**Abstract.** Using resonant x-ray scattering at the Mn K-edge, we have investigated the nature of the charge and lattice modulation in the  $\text{La}_{1-x}\text{Sr}_{1+x}\text{MnO}_4$  ( $x=0.5$  and  $0.6$ ) manganites. Resonant reflections  $(h \pm \varepsilon, h \pm \varepsilon, 0)$  and  $(h \pm 2\varepsilon, h \pm 2\varepsilon, 0)$  of the tetragonal  $I4/mmm$  structure with a modulation vector of  $2\varepsilon=1-x$  were found in the insulating phases of both manganites but the intensity of these reflections is much weaker for  $\text{La}_{0.4}\text{Sr}_{1.6}\text{MnO}_4$ . Resonant x-ray scattering data for the two samples are well explained by the presence of two types of sinusoidal modulations of the oxygen displacements, transverse and longitudinal to the tetragonal [110] direction. The amplitude of the oxygen displacements for any of the modulations decreases with the hole doping, in agreement with the change from a commensurate ( $x=0.5$ ) to an incommensurate ( $x=0.6$ ) ordered phase. The different polarization and azimuthal behaviour of the two sets of resonant reflections rule out any kind of stripe model composed by  $\text{Mn}^{3+}$ -like and  $\text{Mn}^{4+}$ -like charge-ordering. The maximum charge disproportionation among the different Mn atoms in the unit cell is about  $0.15 e^-$  and  $0.04 e^-$  for the  $x=0.5$  and  $x=0.6$  samples, respectively. These results thus confirm the existence of a charge-density-wave ordering in both the commensurate-phase of the half-doped  $\text{La}_{0.5}\text{Sr}_{1.5}\text{MnO}_4$  and the incommensurate-phase of the over-doped  $\text{La}_{0.4}\text{Sr}_{1.6}\text{MnO}_4$  manganites.

### 1. Introduction

In recent years, a large number of studies have been performed on the charge-orbital ordering (COO) of  $e_g$  electrons in mixed-valence manganites. Single-layered  $\text{La}_{1-x}\text{Sr}_{1+x}\text{MnO}_4$  manganites have the tetragonal  $\text{K}_2\text{NiF}_4$ -type fundamental structure based on alternating stacking of  $\text{MnO}_2$  and rock-salt type  $(\text{La,Sr})_2\text{O}_2$  layers. In this system, the concentration of  $e_g$  electrons on the Mn sites ( $n_e$ ) can be described as  $1-x$  above  $x=0.5$  [1,2] and it exhibits the formation of superstructures that have been related to the ordering of charge and orbital of these  $e_g$  electrons at low temperatures, as well as other  $\text{RE}_{1-x}(\text{Sr/Ca})_x\text{MnO}_3$  (where RE stands for rare earth) manganites. The superlattice reflections have been observed for any  $0.5 \leq x \leq 0.67$  [1,2] doping level, or commensurate and incommensurate  $e_g$  electron concentration of  $0.33 \leq x \leq 0.5$ . The wave vector of the structural modulation can be described by  $\mathbf{q}=(1-x)\mathbf{a}^*$ , where  $\mathbf{a}^*$  is the reciprocal lattice vector. For  $x=0.5$  (i.e. with a formal valence of  $\text{Mn}^{+3.5}$ ), the low temperature insulating phase has been long described in terms of stripes of localized charges at atomic sites, where the  $\text{Mn}^{+3.5}$  is split between  $\text{Mn}^{3+}$  ions surrounded by Jahn-



Teller oxygen distorted octahedra and  $\text{Mn}^{4+}$  ions at undistorted sites following a checkerboard pattern [3]. However, we have recently shown that the COO transition in  $\text{La}_{0.5}\text{Sr}_{1.5}\text{MnO}_4$  originates from the structural transition that lowers the crystal symmetry from the tetragonal  $I4/mmm$  to the orthorhombic  $Cmcm$  driven by the condensation of three phonon modes acting on the oxygen atoms [4]. The condensation of these modes establishes the checkerboard ordering of two different Mn sites, the charge disproportionation between them being about 0.2 electrons. For  $x > 0.5$ , incommensurate COO occurs and recent works have produced conflicting evidence about the nature of this incommensurate superstructure, because some studies are supporting a stripe model with charges localized at the atomic Mn sites [5] and others are indicating the formation of a charge-density wave with a periodic modulation of charge density at the atomic Mn sites [6]. The results of our resonant x-ray scattering study in  $\text{La}_{0.4}\text{Sr}_{1.6}\text{MnO}_4$  [7,8] point out to the charge-density-modulation picture due to the presence of oxygen displacements sinusoidal-modulated along and perpendicular to the tetragonal [110] direction.

In the present paper, we show that the resonant x-ray scattering data at the Mn K-edge of the superlattice reflections in single-layered  $\text{La}_{1-x}\text{Sr}_{1+x}\text{MnO}_4$  for all doping levels  $x \geq 0.5$  are consistent with the description in terms of charge-density waves, even at commensurate doping.

## 2. Experimental details

Single crystals of  $\text{La}_{0.5}\text{Sr}_{1.5}\text{MnO}_4$  and  $\text{La}_{0.4}\text{Sr}_{1.6}\text{MnO}_4$  were grown by the floating-zone technique. The growing was carried out at 2 bars of  $\text{O}_2$  with a growth speed ranged between 10 and 12 mm per hour [9]. X-ray diffraction measurements on crushed crystals show patterns typical of single phase tetragonal  $I4/mmm$  structure at room temperature. The single crystals were cut and polished in the (110) plane in the tetragonal setting.

Mn K-edge resonant x-ray scattering experiments were performed at the ID20 beam line [10] at the ESRF. The single crystals were mounted in a four-circle vertical diffractometer that is equipped with a closed-cycle helium refrigerator and a Cu (220) crystal analyser for performing  $\sigma$ - $\sigma'$  and  $\sigma$ - $\pi'$  polarization measurements. Energy scans across the Mn K absorption edge were measured and corrected for absorption using the experimental fluorescence. Azimuth scans at the resonance energy were recorded by rotating the sample around the scattering vector  $\mathbf{Q}$ ,  $\varphi=0^\circ$  for  $\sigma$  polarization vector parallel to the tetragonal [-110] direction. Theoretical calculations of the anomalous atomic scattering factor tensors as a function of the photon energy for the different crystallographic Mn sites were carried out using the FDMNES code [11].

## 3. Results and discussion

The low temperature phase in the two studied single-layered manganites is no longer tetragonal but orthorhombic, whose unit cell is metrically related to the tetragonal one as  $\sqrt{2}a_t \times \sqrt{2}a_t \times c_t$  ( $a_t$  and  $c_t$  being the tetragonal lattice parameters). From here on, we refer to this small orthorhombic cell for comparison purpose. However, the superstructure cell for the  $\text{La}_{0.5}\text{Sr}_{1.5}\text{MnO}_4$  sample with a commensurate doping level of  $x=0.5$  is doubled along the orthorhombic  $a_o$ -axis (tetragonal [110]) whereas for the  $\text{La}_{0.4}\text{Sr}_{1.6}\text{MnO}_4$  sample with an incommensurate concentration of  $x=0.6$ , it becomes commensurate with five cells along the  $a_o$ -axis. The formation of these superstructures is clearly confirmed by the appearance of resonant super-lattice ( $h \pm \varepsilon$ ,  $h \pm \varepsilon$ , 0) and ( $h \pm 2\varepsilon$ ,  $h \pm 2\varepsilon$ , 0) reflections in the tetragonal setting with a modulation vector  $2\varepsilon=1-x$ . Figure 1 compares the energy dependences of some of these characteristic reflections of the superstructures of both  $\text{La}_{0.5}\text{Sr}_{1.5}\text{MnO}_4$  and  $\text{La}_{0.4}\text{Sr}_{1.6}\text{MnO}_4$  samples. The (1.4, 1.4, 0) and (1.6, 1.6, 0) reflections in the  $x=0.6$  sample show the same energy and moderate azimuthal dependence as the (1.5, 1.5, 0) reflection in the  $x=0.5$  sample, as displayed in Fig. 1(a). In the  $\sigma$ - $\sigma'$  polarization channel, both reflections display non-resonant and resonant scattered intensities. The major difference between the two samples concerns the intensity of these superlattice reflections. The non-resonant (Thomson) scattering is about 100 times stronger for the (1.5, 1.5, 0) reflection than for the (1.4, 1.4, 0) and (1.6, 1.6, 0) ones. Since the non-resonant scattering is caused by the atomic displacements breaking the tetragonal symmetry, these

displacements might be significantly larger in the  $x=0.5$  sample and decrease with the hole doping. On the other hand, the energy spectrum of both,  $(1.75, 1.75, 0)$  and  $(1.8, 1.8, 0)$  reflections corresponding to the  $x=0.5$  and  $x=0.6$  samples, respectively, shows similar clear resonant feature in the  $\sigma\text{-}\pi'$  polarization channel, without the non-resonant signal. This indicates that these reflections are forbidden by symmetry and they shall be classified as anisotropy of the tensor of susceptibility (ATS) reflections [12]. Figure 1(b) also shows the same strong azimuthal dependence of  $\pi$  period for the two forbidden reflections. These ATS reflections are permitted due to the presence of a distortion of the  $\text{MnO}_6$  octahedron. The fact that the  $(1.8, 1.8, 0)$  reflection in the  $x=0.6$  sample is reminiscent of the  $(1.75, 1.75, 0)$  reflection in the half-doped sample suggests that a similar distortion of the  $\text{MnO}_6$  octahedron occurs for both compositions. However, the intensity of the  $(1.75, 1.75, 0)$  reflection on resonance is also one order of magnitude stronger than that of the  $(1.8, 1.8, 0)$  one, which indicates that the distortion is smaller for the incommensurate structural modulation.

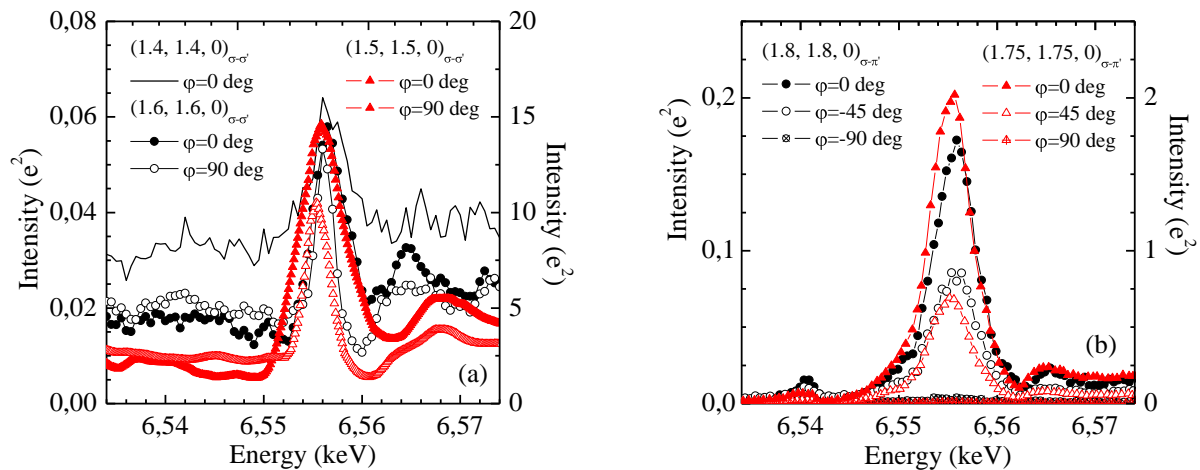


**Figure 1.** (a) Comparison of the energy dependence of the  $(1.4, 1.4, 0)$  and  $(1.6, 1.6, 0)$  reflections for  $\text{La}_{0.4}\text{Sr}_{1.6}\text{MnO}_4$  and the  $(1.5, 1.5, 0)$  reflection for  $\text{La}_{0.5}\text{Sr}_{1.5}\text{MnO}_4$  at  $T=80$  K close to the Mn K-edge in the  $\sigma\text{-}\sigma'$  polarization channel for different azimuthal angles. (b) Comparison of the energy dependence of the  $(1.8, 1.8, 0)$  forbidden reflection for  $\text{La}_{0.4}\text{Sr}_{1.6}\text{MnO}_4$  and the  $(1.75, 1.75, 0)$  forbidden reflection for  $\text{La}_{0.5}\text{Sr}_{1.5}\text{MnO}_4$  at  $T=80$  K close to the Mn K-edge in the  $\sigma\text{-}\pi'$  polarization channel for different azimuthal angles.

The resonant x-ray scattering data point to a structural modulation for the incommensurate  $x=0.6$  sample that seems to be the same as for the commensurate  $x=0.5$  sample, except for the magnitude of the atomic displacements. Therefore, we can consider two different models to simulate the energy, azimuthal and polarization dependence of the intensity of the reported superlattice reflections: (a) the bimodal charge-stripe model with two different Mn sites and (b) the sinusoidal-lattice modulation model with either two or five types of Mn sites for the  $x=0.5$  and  $x=0.6$  samples, respectively. In the case of the  $x=0.6$  sample, the two possible bimodal charge-stripe models cannot explain the lack of  $\sigma\text{-}\sigma'$  and  $\sigma\text{-}\pi'$  intensity for the  $(h\pm 0.2, h\pm 0.2, 0)$  and  $(h\pm 0.4, h\pm 0.4, 0)$  reflections, respectively [7,8]. Thus, we propose the presence of sinusoidal-lattice modulations in the low-temperature insulating phases of both commensurate and incommensurate single-layered  $\text{La}_{1-x}\text{Sr}_{1+x}\text{MnO}_4$  ( $x \geq 0.5$ ) manganites. Since the terms in the Mn anomalous atomic scattering tensor ( $f_{\text{Mn}}^{\alpha\beta}$ ) are mainly determined by the local structure around the Mn atom, a modulation of the oxygen atoms in the  $\text{MnO}_6$

octahedron will induce the same kind of modulation for  $f_{Mn}^{\alpha\beta}$ . In the present case, a longitudinal modulation of the oxygen atoms along the  $a_o$ -axis given by  $\Delta x = \Delta x_0 \cos(2\pi \times n \times 2\varepsilon)$ ,  $n$  being the position of the oxygen atom in the super-cell; the same kind of modulation acting on the apical oxygen atoms (along the  $c_o$ -axis) and a transverse modulation along the  $b_o$ -axis given by  $\Delta y = \Delta y_0 [\cos(2\pi \times n \times \varepsilon) + \sin(2\pi \times n \times \varepsilon)]$  are used. In Fig. 2, we show this superstructure model, with either two or five kinds of  $MnO_6$  octahedra, for  $La_{0.5}Sr_{1.5}MnO_4$  and  $La_{0.4}Sr_{1.6}MnO_4$ , respectively.

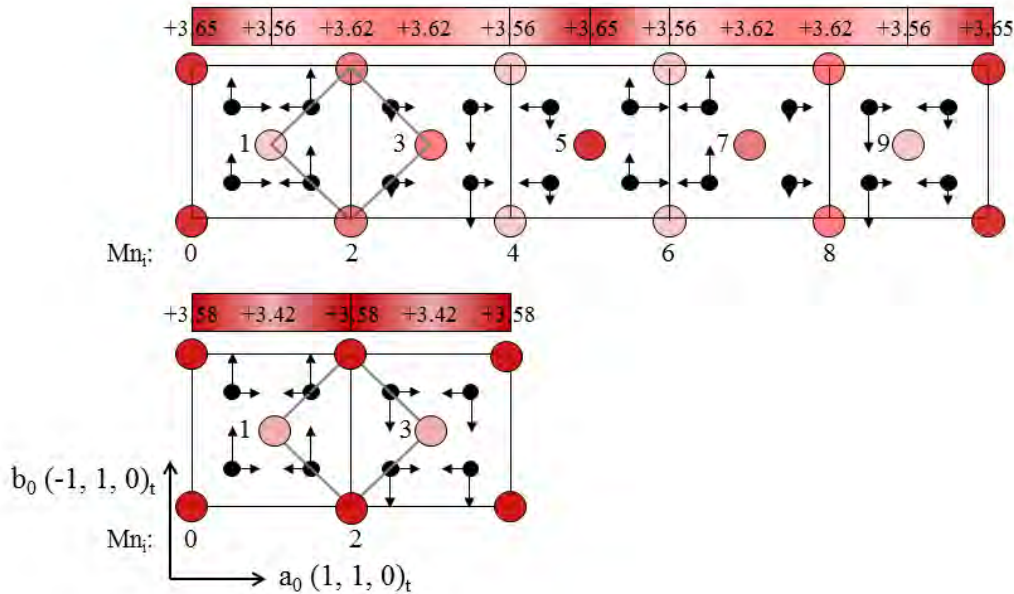


**Figure 2.** Proposed superstructure models for  $x=0.5$  (lower panel) and  $x=0.6$  (upper panel) showing longitudinal and transverse oxygen modulations in the orthorhombic  $a_0$ - $b_0$  plane. The respective sinusoidal Mn valence modulation as a function of position is also indicated.

We have then calculated the Mn anomalous atomic scattering tensor ( $f_{Mn}^{\alpha\beta}$ ) for each of the non-equivalent  $MnO_6$  octahedra using the FDMNES code [11] for a cluster radius of about 5 Å and taking into account the modulation of the  $MnO_6$  distortion amplitude along the three orthorhombic crystallographic axes as described above. Only the diagonal  $f_{xx}$ ,  $f_{yy}$  and  $f_{zz}$  components as well as the out-of-diagonal  $f_{xy}$  components of the anomalous atomic scattering tensor are found to be different from zero. The structure factors of the orthorhombic reflections  $(h', 0, 0)$  with  $h'=4(h\pm 0.5)$  [or  $h'=4(h\pm 0.25)$ ] for  $x=0.5$  and  $h'=10(h\pm 0.4)$  [or  $h'=10(h\pm 0.2)$ ] for  $x=0.6$  are given by the following expression,  $F(h', 0, 0) = \sum_p f_{Mnp}^{\alpha\beta} \exp(i \cdot 2\pi \cdot h' \cdot x_{Mnp})$ , where  $x_{Mnp}$  is the position of the Mn atom along

the  $a_0$ -axis. In the model of the commensurate half-doped sample,  $x_{Mnp} = 0.25 \cdot p$  ( $p=0, 1, 2, 3$ ) whereas in the incommensurate  $x=0.6$  sample,  $x_{Mnp} = 0.1 \cdot p$  ( $p=0, 1, 2, 3, 4, 5, 6, 7, 8, 9$ ). This formulation reproduces well the observed azimuthal and polarization dependencies [7, 8]. Fits to the scattered intensities allow us to obtain the maximum distortions for the longitudinal, transverse and apical modulations as well as the maximum charge disproportionation among the different Mn atoms (see figure 2). Both, oxygen displacements and charge disproportionation strongly decrease with hole doping in agreement with the experimental observation of much weaker superstructure reflections in the  $x=0.6$  sample.

Finally, the intensity of both types of superstructure reflections decreases with increasing temperature and vanishes at  $T_{CO} \sim 230$  K for  $La_{0.5}Sr_{1.5}MnO_4$  and 240 K for  $La_{0.4}Sr_{1.6}MnO_4$ , as shown in Fig. 3. This indicates that the two types of reflections are correlated with the occurrence of the

orthorhombic distortion. However, some differences are observed in the temperature evolution of the intensity between the super-lattice and the forbidden reflections close to  $T_{CO}$ . The slightly different temperature dependence might be related to the hierarchy of the longitudinal and transverse structural modulations driven by the phase transition.

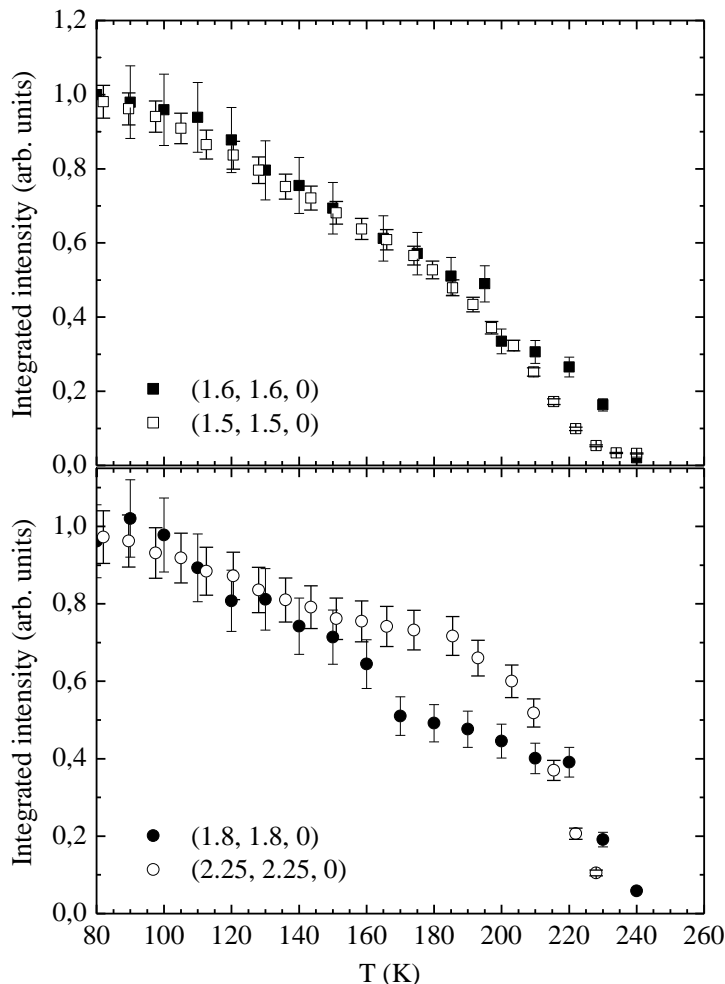


**Figure 3.** Integrated intensities of the  $(h\pm\varepsilon, h\pm\varepsilon, 0)$  and  $(h\pm 2\varepsilon, h\pm 2\varepsilon, 0)$  superstructure peaks with  $2\varepsilon=1-x$  as a function of temperature for the two samples with doping  $x=0.5$  (open symbols) and  $x=0.6$  (filled symbols).

In summary, this resonant x-ray scattering study demonstrates the occurrence of  $(h\pm\varepsilon, h\pm\varepsilon, 0)$  and  $(h\pm 2\varepsilon, h\pm 2\varepsilon, 0)$  superstructure reflections associated to the tetragonal to orthorhombic structural transitions in the  $\text{La}_{1-x}\text{Sr}_{1+x}\text{MnO}_4$  ( $x \geq 0.5$ ) manganites with  $2\varepsilon=1-x$ . Regardless of the commensurate ( $x=0.5$ ) or incommensurate ( $x=0.6$ ) character of the super-structural order,  $(h\pm 2\varepsilon, h\pm 2\varepsilon, 0)$  reflections originate from sinusoidal oxygen motions longitudinal to the modulation direction whereas  $(h\pm\varepsilon, h\pm\varepsilon, 0)$  reflections arise from sinusoidal oxygen motions transverse to the modulation direction. The different energy, polarization, azimuthal and temperature dependencies shown by the two types of superstructure reflections confirm that the  $2\varepsilon$  modulation does not correspond to the second harmonic of the  $\varepsilon$  modulation. Therefore, the continuous charge-orbital density wave model gives a better description for the low temperature ordered phases in single-layered  $\text{La}_{1-x}\text{Sr}_{1+x}\text{MnO}_4$  for all doping levels  $x \geq 0.5$  than any charge-stripe model.

## References

- [1] Laroche S, Metha A, Kaneko N, Mang P K, Panchula A F, Zhou L, Arthur J and Greven M 2001 *Phys. Rev. Lett.* **87** 095502
- [2] Laroche S, Metha A, Lu L, Mang P K, Vajk O P, Kaneko N, Lynn J W, Zhou L and Greven M 2005 *Phys. Rev. B* **71** 024435
- [3] Murakami Y, Kawada H, Kawata H, Tanaka M, Arima T, Moritomo Y and Tokura Y 1998 *Phys. Rev. Lett.* **80** 1932
- [4] Herrero-Martín J, Blasco J, García J, Subías G and Mazzoli C 2011 *Phys. Rev. B* **83** 184101
- [5] Ulbrich H, Senff D, Steffens P, Schumann O J, Sidis Y, Reutler P, Revcolevschi A and Braden M 2011 *Phys. Rev. Lett.* **106** 157201
- [6] Arao M, Inoue Y, Toyoda K and Koyama Y 2011 *Phys. Rev. B* **84** 014102
- [7] García J, Herrero-Martín J, Subías G, Blasco J, Andreu J S and Sánchez M C 2012 *Phys. Rev. Lett.* **109** 107202
- [8] García J, Herrero-Martín J, Subías G, Blasco J and Sánchez M C 2013 *Journal of Physics: Conference Series* **430** 012107
- [9] Blasco J, Sánchez M C, García J, Stankiewicz J and Herrero-Martín J 2008 *J. Cryst. Growth* **310** 3247
- [10] Paolasini L, Detlefs C, Mazzoli C, Wilkins S, Deen P P, Bombardi A, Kernavanois N, de Bergevin F, Yakhov F, Valade J P, Breslavetz I, Fondacaro A, Pepellin G and Bernard P 2007 *J. Synchrotron Radiat.* **14** 301
- [11] Joly Y 2001 *Phys. Rev. B* **63** 125120
- [12] Dmitrienko V E, Ishida K, Kirfel A and Ovchinnikova E N 2005 *Acta Crystallogr. Sect. A* **61** 481